

## Application of the Island Blister Test for Thin Film Adhesion Measurement\*

MARK G. ALLEN and STEPHEN D. SENTURIA,

Microsystems Technology Laboratories, Massachusetts Institute of Technology, Cambridge, MA 02139 U.S.A.

(Received July 21, 1988; in final form February 10, 1989)

The island blister test has recently been proposed as an adhesion test which allows the peel of thin, well-adhered films without exceeding the tensile strength of the film. The island blister test site is a modification of the standard blister test site, consisting of a suspended membrane of film with an "island" of substrate at the film center. The membrane support and island are secured to a rigid plate and the film is pressurized, peeling the film inward off the island. A model for this inward or "annular" peel indicates that even for systems of good adhesion, peel can be initiated at low enough pressures to prevent film failure by making the center island sufficiently small relative to the size of the film.

We have fabricated island blister test sites using micromachining techniques and have used them to measure the debond energy of polymer films on various substrates. The peel data obtained from these island sites match well to the behavior predicted by a simple fracture mechanics analysis. This paper reports the fabrication of the island test sites, the experimental verification of the test, and the results of application of the test to polyimide films on metallic and polymeric substrates.

KEY WORDS adhesion; island blister geometry; peeling of thin films; polyimide/metal adhesion; polyimide/polyimide adhesion; debond energy

### INTRODUCTION

Quantitative measurement of the adhesion and mechanical properties of polymer films is a subject which has received much attention.<sup>3-5</sup> Recently, with the advent of polymer films in microelectronics, the need to measure accurately *in-situ* the mechanical properties and adhesion of polymer films as thin as 2  $\mu\text{m}$  has arisen. Many techniques have been developed and/or adapted from thick film techniques to perform the mechanical property measurement;<sup>5-7</sup> however, there exist few

\* Presented at the 35th Sagamore Army Materials Research Conference, Manchester, New Hampshire, U.S.A., June 26-30, 1988.

Portions of this work have been presented at the 1988 Adhesion Society meeting, Charleston, SC,<sup>1</sup> and the 1988 SPE ANTEC meeting, Atlanta, Georgia.<sup>2</sup>

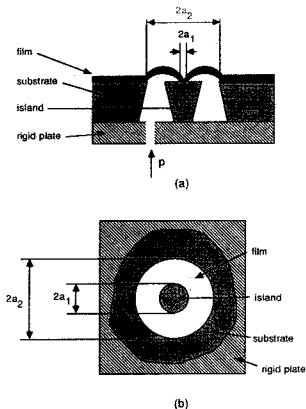


FIGURE 1 (a) Cross section of the island blister structure, where  $a_2$  is the radius of film still adhered to the center island,  $a_1$  is the outer radius of the membrane (a constant),  $\beta = a_2/a_1$ ,  $p$  is the applied pressure. (b) Top view of the island blister structure.

In addition to overcoming the tensile strength limit of these films, it is important to be able to measure the adhesion between film layers. The adhesion of polymer layers is extremely important in many integrated-circuit multilevel-metal interconnect schemes. Cracks between layers can result in moisture ingress and corrosion of metal lines, leading to long-term device reliability problems. In addition, catastrophic delamination (for example, induced by film stress) can result in the sudden and immediate failure of the device. In spite of the importance of interlayer adhesion, few tests are available which can measure quantitatively and *in-situ* the energy necessary to debond these films. Preliminary work has focused primarily on the peel test. However, the peel test suffers from two shortcomings which limit its utility in this application. First, loading the sample is difficult; grasping one layer of film while keeping the others adhered can be a problem. Second, the films may again be tensile strength limited. The island blister can be used to overcome both the loading problem and tensile strength limit. This paper reports experimental verification of the island blister test as proposed previously and illustrates the application of the test through two

techniques which quantitatively measure the adhesion of thin, well-adhering polymer films.

The major reason for this is that thin, well-adhered polymer films often are *tensile-strength limited* when subjected to various adhesion tests. That is, upon attempting to remove the film from the substrate in a controlled manner, the film tears before it peels.<sup>8</sup> Almost every attempted solution to this problem involves strengthening the film in some way. For example, in the standard 90° peel test, a very thick layer of polymer is often built up so that it can be peeled without tearing.<sup>9,10</sup> The problems inherent in this method are twofold. First, it is not clear that the adhesive strength (*i.e.*, the "interfacial adhesive strength") is the same for a thick film and a thin film of the same material. Second, the peel strength (the observable quantity in the peel experiment) may change drastically as the film thickness increases.<sup>11</sup> Thus, it is desirable to investigate the feasibility of a test which can be adapted to thin films without modifying them in any way.

A closely related test to the peel test is the blister test.<sup>12</sup> In this test, a film is pressurized through a hole in the substrate by a fluid (liquid or gas) until it begins to peel from the substrate. If the blister geometry is known, the debond energy can be calculated from the pressure at which peel initiates.<sup>13-15</sup> It has been demonstrated that blister test sites can be fabricated using materials of importance in microelectronics. Hinkley<sup>16</sup> has succeeded in fabricating suspended polymer films on silicon wafers using a non-lithographic fabrication process. However, the blister test suffers from the tensile strength limitation mentioned previously; if films are thin and/or well-adhering, blisters may burst before peel can be initiated. In spite of this, the blister test offers several ways around the tensile strength limit. These will be discussed below.

One method which has been proposed to overcome this limit is the "constrained blister test".<sup>17,18</sup> In this test, the growing blister is constrained in the vertical direction by placing a plate over it. The plate prevents large deflections in the vertical direction, allowing large pressures to be applied to the blister without tearing the film. The initial measurements using this test were done with adhesive tapes. However, it is possible that films which fail due to defect formation (for example, solvent-cast films as opposed to tapes) will still fail in the constrained blister test, which is of maximum utility for films which fail due to exceeding the maximum strain of the film.

The structure we propose to overcome the tensile strength limit is called the "island blister".<sup>19</sup> The island blister is a modification of the standard blister site in that the suspended membrane of film has an "island" of substrate still attached at its center. The island and the substrate are both fastened to a rigid plate and pressure is applied as in the standard blister (Figure 1). Film peeling will now occur only off the center island. It can be shown<sup>15,19</sup> that the pressure necessary to initiate peel can be made low compared to the tensile strength of the film simply by making the center island sufficiently small. Thus, the tensile strength limit of the film can be overcome geometrically. This structure does not suffer from the drawbacks of the constrained blister test in that relatively low pressures are used to initiate and sustain peel; therefore, the issue of defect-induced failure is not as important.

experimental cases: two different types of polyimide on aluminum substrates and the effect of solvent soaking on polyimide-polyimide adhesion.

### THEORETICAL

In a recent paper<sup>15</sup> we presented the theoretical justification for the island blister test. The blister structure was modelled using an energy minimization approach combined with linear elastic fracture mechanics. Modeling the island structure as a circular adhered film area on an island at the center of a circular suspended membrane the load-deflection behavior of which is dominated by residual stress, it can be shown that the pressure to initiate peel ( $p_c$ ), the debond energy of the film ( $\gamma_a$ ), and the radius of film still adhered to the island ( $a_1$ ) are related by (Figure 1):

$$\gamma_a = \frac{\rho_c^2 a_1^2}{32 \sigma_0 t} f(\beta) \quad (1)$$

where  $t$  is the film thickness,  $a_2$  is the radius of the suspended film,  $\sigma_0$  is the residual stress in the film,  $\beta$  is the ratio  $a_2/a_1$ , and  $f(\beta)$  is a function given by:

$$f(\beta) = \left[ \frac{\beta^2 - 1}{\ln \beta} - 2 \right]^2 \quad (2)$$

It should be emphasized that Eqs (1) and (2) are valid only when the strain energy induced in the film due to deflections against the residual stress  $\sigma_0$  is large compared to the additional strain energy induced in the film due to stretching (*i.e.*, if  $\sigma_0$  is large enough).<sup>15</sup>

It can be seen from Eqs 1 and 2 that  $p_c$  decreases as the size of the center island decreases (*i.e.*, as  $\beta$  increases). In fact, if the size of the center island is arbitrarily small, then for a given  $\gamma_a$ ,  $p_c$  can be made arbitrarily low (*i.e.*, less than the film's tensile strength limit). This is the fundamental advantage of the island blister geometry.

Once the film has peeled, a suspended membrane of the film is formed (Figure 2). The residual stress in the film can be determined *in-situ* by a measurement of the load-deflection characteristics of the membrane.<sup>20,21</sup> It can be shown that the deflection at the center of a square membrane in response to the applied pressure is given by:

$$\left( \frac{Et}{a^2} \right) d^3 + \left( \frac{1.66t\sigma_0}{a^2} \right) d = 0.547p, \quad (3)$$

where  $p$  is the applied pressure,  $E$  is Young's modulus,  $\sigma_0$  is the residual stress in the film,  $2a$  is the edge length of the square,  $t$  is the film thickness, and  $d$  is the deflection at the center of the membrane. If a set of pressure-deflection data are taken, a plot of  $p/d$  versus  $d^2$  is linear with slope proportional to Young's modulus and intercept proportional to the residual stress.<sup>21</sup> Thus, the debond energy of the film can be determined from a combination of island peel and load-deflection measurements.

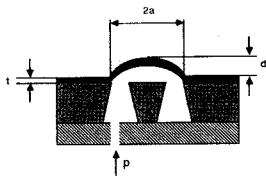


FIGURE 2 Structure for residual stress measurement. A square suspended membrane of thickness  $t$  and edge length  $2a$  undergoing a deflection  $d$  at its center in response to an applied pressure  $p$ .

#### FABRICATION AND MEASUREMENT

In order for the island blister test to be generally applicable, it is necessary to be able to make the quantity  $\beta$ , the ratio of outer to inner radius, arbitrarily large. For many macroscopic applications, this can be most easily achieved by fixing the island radius to some convenient size and increasing the outer film radius to the point that the film can be peeled. However, for microelectronic applications, the outer film size is limited by the desire to fit test sites on a silicon wafer. In this case, it is necessary to have the ability to make the island arbitrarily small. However, the island must not be so small that it cannot be fastened down to the rigid substrate. In other words, while it may be necessary for the island to be *microscopic* in size so that the tensile strength of the film will not be exceeded in measuring adhesion, it is necessary for the island to be *macroscopic* in size in order that it be fastened down prior to measurement. This problem is overcome by using a macroscopic island and covering the island with a "release layer." The release layer can be either a material to which the film does not adhere well or two layers which do not adhere well to each other. A microscopic hole is patterned in the center of the release layer which exposes the adherend on the island, and the film is deposited. Using this scheme, only the small area of the film where the release layer has been removed will be actually adhered. When pressure is applied, the film will easily peel from the release layer and stop when it reaches the exposed adherend. Thus, a microscopic adhered area has been achieved on a macroscopic island. We have used both release layer techniques successfully, although in this paper we will report only the single-layer technique.

As we are interested in materials used in microelectronic fabrication, we have used bulk micromachining techniques to make island blister sites on silicon wafers. One of the advantages of using silicon wafers is the ability to etch holes anisotropically in the wafer using various etchants which etch only along certain crystal planes in the silicon. The use of these etchants allows more precise control of geometries than standard isotropic etchants; however, their use also results in

square diaphragms rather than the circular diaphragms which have been modeled above. Analogous to the load-deflection behavior of circular *versus* square diaphragms, however, this should change only the absolute value of measured debond energy (*i.e.*, the constant in the denominator of Eq. (1)), but not the functional form of Eq. (1). This assumption is confirmed by data which will be presented later in the paper.

Island blister test sites are fabricated using micromachining techniques.<sup>21</sup> On each die (blister site), a  $5\ \mu\text{m}$  thick square diaphragm with an island of silicon at the center is etched in a (100) silicon wafer from the back using a silicon dioxide etch mask, a  $5\ \mu\text{m}$   $p^+$  diffusion of boron as an etch stop, and 50% hydrazine in water as the anisotropic etchant. There may be anywhere from four to nine die per two inch wafer. The diaphragms may range from six to ten millimeters on a side, while the islands are typically one millimeter on a side. The silicon dioxide etch mask is stripped in hydrofluoric acid and a film of the adherend of interest is then deposited and patterned so as to leave an adherend "pad" over each of the islands. A release layer for the film is then deposited and patterned so as to expose only a small portion of the adherend pad, yielding an initial adhered radius  $a_1$  which can, therefore, be as small as several microns in diameter if desired. For this work, an initial adhered radius of  $200\ \mu\text{m}$  was used. The thin film of interest is then deposited on the wafer, contacting the adherend pad through the hole in the release layer. The  $5\ \mu\text{m}$  silicon diaphragm is then removed using a backside  $\text{SF}_6$  plasma etch to form the suspended membrane portion of the test site. Figure 3 shows the full fabrication sequence for the island blisters.

The wafer and islands were secured to a type 304 stainless steel plate using commercial epoxy, and the plate was placed in a test apparatus.<sup>22</sup> Pressure was

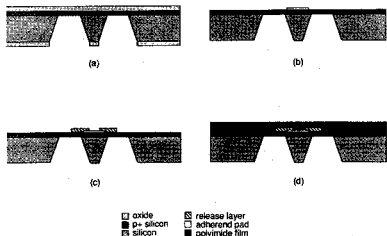


FIGURE 3 Fabrication sequence of island blister structures. (a) island pattern in silicon; (b) after patterning of adherend pad; (c) after patterning of (optional) release layer; (d) final structure (note: to scale, actual dimensions in text).

square diaphragms rather than the circular diaphragms which have been modeled above. Analogous to the load-deflection behavior of circular *versus* square diaphragms, however, this should change only the absolute value of measured debond energy (*i.e.*, the constant in the denominator of Eq. (1)), but not the functional form of Eq. (1). This assumption is confirmed by data which will be presented later in the paper.

Island blister test sites are fabricated using micromachining techniques.<sup>21</sup> On each die (blister site), a  $5\ \mu\text{m}$  thick square diaphragm with an island of silicon at the center is etched in a (100) silicon wafer from the back using a silicon dioxide etch mask, a  $5\ \mu\text{m}$   $p^+$  diffusion of boron as an etch stop, and 50% hydrazine in water as the anisotropic etchant. There may be anywhere from four to nine die per two inch wafer. The diaphragms may range from six to ten millimeters on a side, while the islands are typically one millimeter on a side. The silicon dioxide etch mask is stripped in hydrofluoric acid and a film of the adherend of interest is then deposited and patterned so as to leave an adherend "pad" over each of the islands. A release layer for the film is then deposited and patterned so as to expose only a small portion of the adherend pad, yielding an initial adhered radius  $a_1$  which can, therefore, be as small as several microns in diameter if desired. For this work, an initial adhered radius of  $200\ \mu\text{m}$  was used. The thin film of interest is then deposited on the wafer, contacting the adherend pad through the hole in the release layer. The  $5\ \mu\text{m}$  silicon diaphragm is then removed using a backside  $\text{SF}_6$  plasma etch to form the suspended membrane portion of the test site. Figure 3 shows the full fabrication sequence for the island blisters.

The wafer and islands were secured to a type 304 stainless steel plate using commercial epoxy, and the plate was placed in a test apparatus.<sup>22</sup> Pressure was

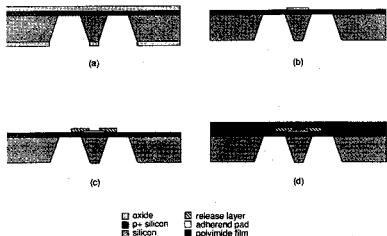


FIGURE 3 Fabrication sequence of island blister structures. (a) island pattern in silicon; (b) after patterning of adherend pad; (c) after patterning of (optional) release layer; (d) final structure (note: to scale, actual dimensions in text).

applied through holes in the plate, and was measured using a silicon pressure transducer built into the test apparatus. The pressurized blisters were observed in an optical microscope and the pressure at which the film began to peel ( $p_c$ ) was observed as a function of the radius of film still adhered to the island ( $a_1$ ). When the film began to peel, the pressure was lowered until peel ceased. The new  $a_1$  was then measured using the calibrated  $x - y$  stage of the microscope (accurate to approximately  $2 \mu\text{m}$ ), and the pressure raised until the film began to peel again. In this way, a set of  $p_c$  vs.  $a_1$  data could be measured. Once the film peeled completely from the center island, the deflection of the film as a function of pressure was measured by focusing the microscope on the top of the film and using a digital micrometer to measure the deflection of the microscope stage necessary to keep the film in focus.

Two distinct classes of experiments were performed. In the first class, the debond energy of polyimide (thin film) to various metals (adherend pad) was measured. In the second class, the self-adhesion of polyimide layers was measured and the effect of pretreatment of the polyimide layers on the interlayer adhesion was investigated. Each of these experiments will be discussed below.

#### A. Adhesion to Metallic Substrates

Island blister test sites were fabricated as described above up to the stripping of the masking oxide in hydrofluoric acid. A  $1500 \text{ \AA}$  thick film of aluminum was then deposited in an electron beam evaporator at a rate of  $25 \text{ \AA}/\text{sec}$ . The polyimide of interest (see below) was then spin cast and cured. The  $5 \mu\text{m}$  silicon diaphragm was removed using a backside  $\text{SF}_6$  plasma etch and the aluminum was removed from the membrane area using a phosphoric-acetic-nitric acid solution to form the island blister. Two types of polyimide were tested, a pyromellitic dianhydride—oxydianiline formulation (PMDA-ODA) and a benzophenonetetracarboxylic dianhydride—oxydianiline/metaphenylenediamine formulation (BTDA-ODA/MPDA). The polyimides were spun as their polyamic acid precursors from solution in *N*-methyl-2 pyrrolidone (NMP) in multiple coats at 4000 rpm for 90 seconds, with a 15-minute prebake in air at  $150^\circ\text{C}$  between coats. The PMDA-ODA polyimide was applied in three coats and BTDA-ODA/MPDA polyimide was applied in two coats, so as to yield an after-cure thickness of  $4.5 \mu\text{m}$  for each polyimide. The final cure was carried out in nitrogen at  $400^\circ\text{C}$ .

Five test sites were measured, three of PMDA-ODA and two of BTDA-ODA/MPDA. Figures 4 and 5 present the peel data for the two polyimides. The peel data are plotted in accordance with Eqs (1) and (2), with  $a_1^2 f(\beta)$  on the  $y$ -axis and  $\sigma_0 p_c^{-2}$  on the  $x$ -axis. From Eq. (1), such a plot should be a straight line through the origin with slope equal to  $32\gamma_a$ . The residual stress/thickness product used for plotting the data was calculated by a post-peel load-deflection measurement as described above. The thickness was measured using a surface profilometer, allowing the independent calculation of residual stress. Values for thickness, stress, and debond energy of each polyimide are given in Table I. With one exception, the reproducibility of the measurement from site to site was good.



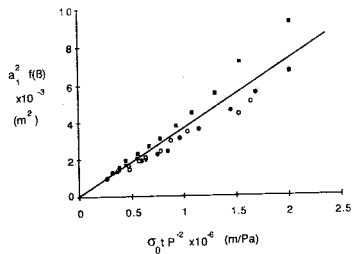


FIGURE 4 Adhesion plot of PMDA-ODA on aluminum (three nominally identical sites).

The PMDA-ODA polyimide has consistently poorer adhesion to aluminum than the BTDA-ODA/MPDA polyimide. This is consistent with previous qualitative observations.<sup>23</sup> The residual stresses measured for polyimide on aluminum are somewhat lower than previously reported values for these same polyimides on silicon dioxide;<sup>21</sup> the effect of the substrate on film residual stress is a topic of current study.

The debond energy inferred from the island blister test (in  $\text{J/m}^2$ ) can be converted to an equivalent  $90^\circ$  peel strength (in  $\text{g/mm}$ ) by dividing by 9.8. For PMDA-ODA, the equivalent peel strength is  $11.1 \text{ g/mm}$ , and for BTDA-

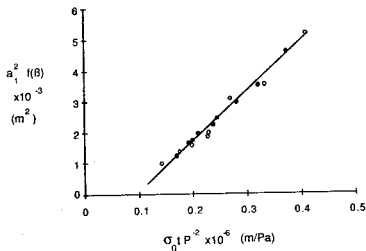


FIGURE 5 Adhesion plot of BTDA-ODA/MPDA on aluminum (two nominally identical sites).

TABLE I  
Summary of adhesion data for polyimide/aluminum experiments

Polyimide	film thickness ( $\mu\text{m}$ )	slope of adhesion plot ( $\text{Pa}\cdot\text{J}/\text{m}$ )	residual stress (MPa)	work of adhesion ( $\text{J}/\text{m}^2$ )
PMDA-ODA	4.5	330000	24.2	94.7
PMDA-ODA	4.5	331000	25.8	89.1
PMDA-ODA	4.5	489000	23.7	143
BTDA-ODA/ MPDA	4.5	2340000	33.0	492
BTDA-ODA/ MPDA	4.5	1670000	24.7	470

ODA/MPDA, the equivalent peel strength is 49 g/mm. These numbers are generally lower than reported  $90^\circ$  peel strengths obtained from thicker films.<sup>9</sup> It is not known whether this experimental discrepancy is due to variations in sample preparation. However, it must be remembered that a peel measurement incorporates dissipative effects (viscoelastic and plastic) as well as debond energy in the peel strength. The fact that dissipative effects are present is shown by the finite peel rate (typically 2–5  $\mu\text{m}/\text{s}$ ) seen in peeling films at constant pressure in the otherwise unstable island blister configuration. Kim<sup>11</sup> has shown that this dissipative term is substantial in the  $90^\circ$  peel test. The smaller peel angle (close to  $0^\circ$ ) of the island blister test, and the fact that these films are typically much thinner than polyimides peeled in the  $90^\circ$  peel configuration, may account for the observed difference in peel strength between the two configurations. We are presently extending the simple peel model of Eqs 1 and 2 to include both dissipative effects and the contribution of the modulus of the film to the  $p_c - \gamma_a$  relationship.

### B. Adhesion of Polyimide Layers

Two types of experiments were carried out. In the first experiment, island blisters using polyimide layers as both adherend and film were fabricated as described below. The first layer was 1  $\mu\text{m}$  of a PMDA-ODA polyimide which had been fully cured at  $400^\circ\text{C}$  for 45 minutes. The second layer was also PMDA-ODA 5.1  $\mu\text{m}$  thick and cured under the same conditions. The interlayer adhesion was then measured using the island blister technique. The second experiment was carried out to test the recent suggestion<sup>24,25</sup> that swelling the first layer in a good solvent (such as N-methyl-2-pyrrolidone, NMP) may improve the interlayer adhesion. Control samples were prepared as described above. Another set of samples was swelled in NMP for 20 or 40 minutes at either  $25^\circ\text{C}$  or  $90^\circ\text{C}$  prior to the application of the second coat. Thus, the dependence of the interlayer adhesion on the time and temperature of the NMP soak could be investigated.

Island blister test sites were fabricated as described above up to the removal of the silicon dioxide etch mask. The wafers were treated with a 0.1% solution of  $\gamma$ -triethoxyaminopropylsilane adhesion promoter in 95% methanol-5% water solution by spin coating at 5000 rpm for 30 seconds. A  $1\ \mu\text{m}$  thick film of PMDA-ODA polyimide was then spin-cast from its polyamic acid precursor in NMP onto the wafer and pre-baked in order to imidize the film partially. The polyimide was then patterned lithographically into  $400 \times 400\ \mu\text{m}$  squares (adherend pads) aligned with the silicon islands using photoresist and a tetramethylammonium hydroxide developer as both the resist developer and polyimide etch. The photoresist was stripped in an acetone/methanol rinse and a low-power oxygen plasma descum, and the resulting polyimide squares (adherend pads) were cured at  $400^\circ\text{C}$  in nitrogen for 45 minutes. A thin ( $100\ \text{\AA}$ ) layer of copper (the release layer) was deposited on the wafer using an electron-beam evaporator and was patterned using a ferric chloride solution into squares which covered the island and adherend pad, but left the central portion of the pad exposed. The polyimide adherend pads (forming the first layer of the interlayer peel structure) were given a short low-power plasma descum and subjected to the NMP soak process described above. The second layer of polyimide was spin-coated and cured at  $400^\circ\text{C}$  in nitrogen for 45 minutes. The supporting silicon diaphragm was then removed as described above to expose the backside of the second polyimide layer and form the island blister.

Peeling of a typical polyimide/polyimide test site for zero soak time is shown in Figure 6. A post-peel load-deflection measurement yielded a  $\sigma_0 t$  product of  $87.1\ \text{Pa m}$  which was used in plotting the adhesion data in accordance with Eq. 1. As can be seen, the data fit the theory quite well, giving a straight line through the origin. From the slope of this line a value for the debond energy of  $94\ \text{J/m}^2$

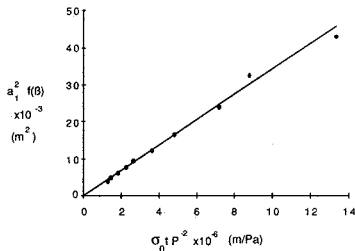


FIGURE 6 Adhesion plot of PMDA-ODA interlayer peel (zero soak time).

TABLE II  
Summary of adhesion data for polyimide interlayer adhesion experiments

(a)  $T = 25^{\circ}\text{C}$ 

Site	Soak time (min)	Adhesion plot slope (Pa J / m)	Stress - thickness product (Pa m)	debond energy ( $\text{J} / \text{m}^2$ )	
1	0	257,000	87.1	94	$90 \pm 13$
2	0	277,100	85.0	99	
3	0	203,100	83.0	77	
4	20	325,300	86.2	118	118
5	40	303,000	90.2	105	$112 \pm 8$
6	40	329,000	92.9	111	
7	40	397,000	103.6	120	

(b)  $T = 90^{\circ}\text{C}$ 

Site	Soak time (min)	Adhesion plot slope (Pa J / m)	debond energy ( $\text{J} / \text{m}^2$ )		
1	10	235,000	82	$105 \pm 23$	
2	10	367,000	127		
3	10	304,000	106		
4	20	241,000	84	$107 \pm 23$	
5	20	374,000	130		

(\*) Nominal stress-thickness product of 90 Pa-m used

was obtained for this test site. All of these sites tested obeyed the behavior predicted by Eqs 1-3.

The data for all the experiments are summarized in Table II. The number of sites tested, conditions of pretreatment of the first layer (if any), slope of the adhesion plot, measured residual stress, and calculated debond energy are all given. For some of the sites, the residual stress was not measured; the nominal value (taken from other sites which had undergone identical deposition and curing of the second layer) was used. Figure 7 displays the data of Table II in a bar graph of debond energy for the various soak times and temperatures.

Although there is considerable scatter in the data, some trends may be observed. There does appear to be a slight increase in debond energy with soak

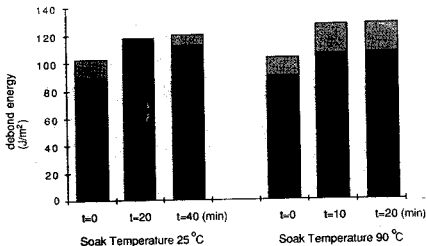


FIGURE 7 Debond energy as a function of NMP soak time and temperature.

time. For example, in the room temperature soak experiments, the highest measured value of the debond energy at zero soak time is lower than the lowest measured value of the debond energy at 40 minutes soak time. In addition, it seems as if increasing the temperature of the soak had a very small enhancing effect on the interlayer adhesion. The highest debond energy was observed for the high temperature soak at long times, although these conditions also resulted in the most scatter in the data. The recent work of Tong<sup>25</sup> indicates that much longer soak times and/or higher soak temperatures for polyimide-polyimide adhesion enhancement are appropriate, from 2-3 days at 21°C to 30-60 minutes at 120°C. We are presently investigating these conditions using the island blister test.

#### CONCLUSIONS

The island blister test, a method for quantitatively measuring the adhesion of thin, well-adhered films has been described. It has been shown that films which are tensile strength limited in ordinary adhesion tests can be peeled using the island blister technique. A model for the test relating critical pressure to the debond energy of the film, developed in a previous paper, has been shown to describe island blister data quite well. In order to demonstrate the utility of the test, two cases were chosen for study: polyimide adhesion to aluminum and polyimide interlayer adhesion. For a 4.5  $\mu\text{m}$  thick PMDA-ODA polyimide on aluminum, the debond energy was measured to be  $109 \pm 34 \text{ J/m}^2$  (3 sites), while for a 4.5  $\mu\text{m}$  thick BTDA-ODA/MPDA polyimide on aluminum, the debond energy was measured to be  $481 \pm 11 \text{ J/m}^2$  (2 sites). For the interlayer adhesion case, the debond energy of PMDA-ODA polyimide layers was measured to be

approximately  $90.5 \text{ J/m}^2$ , although the data were considerably more scattered than the polyimide/metal structures. Soaking of the first polyimide layer in NMP resulted in a slight increase in the interlayer debond energy.

#### Acknowledgement

This work was supported in part by the Semiconductor Research Corporation under contract number 87-SP-080, by E. I. DuPont de Nemours & Co., and by a graduate fellowship from the International Society for Hybrid Microelectronics. Microfabrication was carried out in the Microsystems Technology Laboratories, and in the Microelectronics Laboratory of the MIT Center for Materials Science and Engineering, which is supported by the National Science Foundation under Contract DMR-84-18718. The authors wish to acknowledge helpful discussions with Dr. E. L. Yuan of Dupont on aspects of polyimide adhesion and Dr. H. Brown of IBM on the effects of polyimide swelling on interlayer adhesion.

#### References

1. M. G. Allen and S. D. Senturia, Technical Abstracts, The Adhesion Society 11th annual meeting, p. 61 (1988).
2. M. G. Allen and S. D. Senturia, Proceedings of the 46th Society of Plastics Engineers Annual Technical Conference, p. 997-999 (1988).
3. See, e.g., W. D. Weber and M. R. Gupta, Eds., *Recent Advances in Polyimide Science and Technology* (Society of Plastics Engineers, Mid-Hudson Chapter, 1987).
4. K. L. Mittal, *Electrocomponent Sci. and Tech.* 3, 21 (1976).
5. R. W. Hoffmann, in *Physics of Nonmetallic Thin Films*, C. H. S. Dupey and A. Cachard, Eds., NATO Advanced Study Institutes, vol. B-14 (Plenum, NY, 1976).
6. D. S. Campbell, in *Handbook of Thin Film Technology* (McGraw-Hill, New York, 1970), p. 12-24.
7. P. Geldermans, C. Goldsmith, and F. Bendetti, in *Polyimides—Synthesis, Characterization, and Applications*, K. L. Mittal, Ed. (Plenum, New York, 1984), p. 695.
8. L. B. Rothman, *J. Electrochemical Soc.* 127, 2216 (1981).
9. D. Suryanarayana and K. L. Mittal, *J. Appl. Poly. Sci.* 29, 2039 (1984).
10. R. Narechiana, J. Bruce, and S. Fridmann, *J. Electrochemical Soc.* 132, (1985).
11. K. Kim and J. Kim, *Transactions of the ASME, WA/EEP-3*, 1986.
12. H. Dannenberg, *J. Appl. Poly. Sci.* 5, 125 (1961).
13. M. L. Williams, *J. Appl. Poly. Sci.* 13, 29 (1969).
14. A. N. Gent and L. H. Lewandowski, *J. Appl. Poly. Sci.* 33, 1567-1577 (1987).
15. M. G. Allen and S. D. Senturia, *J. Adhesion* 25, 303-315 (1988).
16. J. A. Hinkley, *ibid.* 16, 115 (1983).
17. M. J. Napolitano, A. Chudnovsky, and A. Moet, *Proceedings of the American Chemical Society Division of Polymeric Materials: Science and Engineering* 57, 755-759 (1987).
18. D. A. Dillard, presentation to the Adhesion Society, February, 1988.
19. M. G. Allen and S. D. Senturia, *Proceedings of the American Chemical Society Division of Polymeric Materials: Science and Engineering* 56, 735-739 (1987).
20. J. W. Beams, in *Structure and Properties of Thin Films*, C. A. Neugebauer, Ed. (John Wiley & Sons, New York, 1959), p. 183-192.
21. M. G. Allen, M. Mehregany, R. T. Howe, and S. D. Senturia, *Appl. Phys. Lett.* 51, 241 (1987).
22. M. G. Allen, S. M. Thesis, Department of Chemical Engineering, Massachusetts Institute of Technology, 1986.
23. E. L. Yuan, private communication.
24. H. R. Brown, A. Yang, and T. P. Russell, presentation to the Materials Research Society (Paper L3.7), December, 1987.
25. H. M. Tong and K. Saenger, presentation to the Materials Research Society (Paper L5.4), December, 1987.